

# We are IntechOpen, the world's leading publisher of Open Access books Built by scientists, for scientists

6,900

Open access books available

186,000

International authors and editors

200M

Downloads

Our authors are among the

154

Countries delivered to

TOP 1%

most cited scientists

12.2%

Contributors from top 500 universities



WEB OF SCIENCE™

Selection of our books indexed in the Book Citation Index  
in Web of Science™ Core Collection (BKCI)

Interested in publishing with us?  
Contact [book.department@intechopen.com](mailto:book.department@intechopen.com)

Numbers displayed above are based on latest data collected.  
For more information visit [www.intechopen.com](http://www.intechopen.com)



# Micro-Electro-Discharge Machining Technologies for MEMS

Kenichi Takahata  
*University of British Columbia, Vancouver  
Canada*

## 1. Introduction

Advances in micromachining techniques have led to the evolution of micro-electro-mechanical systems (MEMS). These techniques are typically based on semiconductor manufacturing processes, which offer various advantages such as batch manufacturing of miniaturized devices and monolithic integration of microelectronics with the devices. Surface micromachining has been used to construct complex microstructures, but since the structural geometries of these microstructures are two-dimensional, their mechanical abilities are often limited. This constraint has been addressed by the use of bulk micromachining techniques that involve etching and deposition processes. Anisotropic wet etching (Sato et al., 1998) and deep reactive ion etching (Laermer & Urban, 2005) have been widely used to create three-dimensional (3-D) geometries in MEMS. However, these processes are severely limited in their material options. As for deposition, electroplating is widely used to form 3-D metallic microstructures, but practical materials are limited to selected metals and alloys. In contrast, certain stainless steels and shape memory alloys have been commonly used for a variety of biomedical and implant devices such as stents and surgical devices. These materials have not been leveraged as much as silicon in MEMS, however, largely because they are not compatible with MEMS fabrication processes. As these examples indicate, there is an explicit gap between the diversity of engineering materials and the ability to use them in the design/ fabrication of MEMS; bridging this gap is expected to create new opportunities in the field.

Micro-electro-discharge machining ( $\mu$ EDM) is a powerful bulk micromachining technique, as it is applicable to any type of electrical conductor, including all kinds of metals and alloys as well as doped semiconductors.  $\mu$ EDM is a non-contact machining technique, hence it can be easily applied to thin, fragile, and/ or soft materials regardless of their mechanical properties. Complex 3-D shapes can be achieved through numerical control (NC) systems with high-precision positioning stages. These unique features and the extensive material base available to  $\mu$ EDM have led to the process being leveraged for industrial applications, such as ink-jet nozzle fabrication (Allen & Lecheheb, 1996), micromachining of magnetic heads for digital VCRs (Honma et al., 1999), and micromechanical tooling (Wada & Masaki, 2005). In recent years, the technique has been increasingly utilized for MEMS fabrication to exploit a broad range of engineering materials that are incompatible with standard MEMS processes, overcoming the common constraint in MEMS, i.e., lack of diversity of bulk materials available for their fabrication (Takahata & Gianchandani, 2007).

Source: Micro Electronic and Mechanical Systems, Book edited by: Kenichi Takahata,  
ISBN 978-953-307-027-8, pp. 572, December 2009, INTECH, Croatia, downloaded from SCIYO.COM

This chapter discusses the basic principles and advanced technologies of  $\mu$ EDM in Subsections 2 and 3, respectively. Subsection 4 describes how the technique has been used to realize various types of MEMS devices, while introducing selected applications it has enabled. The discussion involves not only how  $\mu$ EDM has enabled MEMS but also how MEMS have enabled advanced  $\mu$ EDM processes, which is included in Subsection 3.

## 2. Features and challenges

$\mu$ EDM utilizes pulses of thermomechanical impact induced by a miniaturized electrical discharge generated between a microscopic electrode and a workpiece while both are immersed in dielectric liquid (Masaki et al., 1990). The miniaturized arc discharge, which usually involves a pulse energy of 0.01-10  $\mu$ J with duration of 10-100 ns, is reported to reach a temperature of several 1000s K (Dhanik & Joshi, 2005), locally melting and evaporating the material at the arc spot (Fig. 1). The heat generated by an arc also leads to instant evaporation of the dielectric liquid (typically kerosene-based oil or ultrapure water). This evaporation creates pressure waves that blow the melted material away, leaving a crater-like cavity on the workpiece surface. Machining is performed by repeating this unit removal by a single pulse at high frequencies. Burr-free, high-aspect-ratio (>20) micromachining achieved through this technique can produce features of a few microns with submicron tolerances. High-precision machining of high-aspect-ratio cylindrical electrodes with diameters of 3-300  $\mu$ m, usually of tungsten or its alloy, is available using a  $\mu$ EDM technique called wire electro-discharge grinding, or WEDG (Masuzawa et al., 1985).

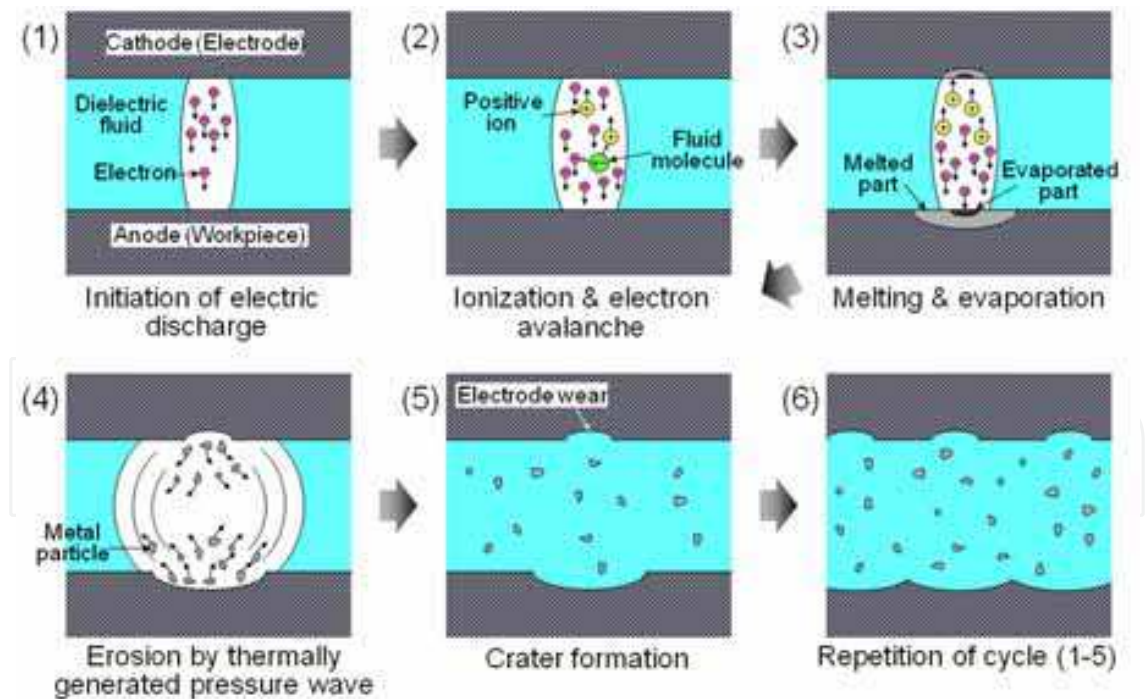


Fig. 1.  $\mu$ EDM principle illustrated.

3-D microstructures are machined with NC of the relative position between an electrode and a workpiece. An example of a commercial  $\mu$ EDM machine equipped with 3-axis stages with 100-nm resolution and a WEDG unit is shown in Fig. 2, along with a typical machining method for arbitrary shapes using a cylindrical electrode, which is usually rotated during

the process. Figure 3 shows a sample structure fabricated by a prototype 5-axis system with two rotational mechanisms (Takahata et al., 1997), demonstrating real 3-D micromachining. Another related technique is wire  $\mu$ EDM, where brass wire is typically used as an electrode that is scanned to cut structures out from the workpiece (Ho et al., 2004).

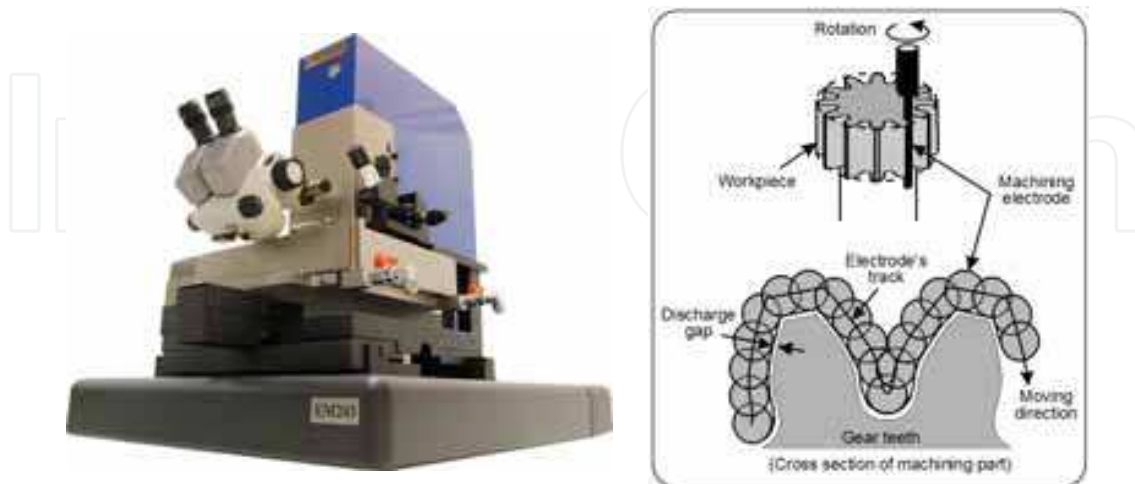


Fig. 2. (a: left) A commercially available  $\mu$ EDM machine (EM203, SmalTec International, USA, image courtesy SmalTec); (b: right) a method for creating arbitrary shapes in a bulk-metal workpiece using a conventional cylindrical electrode (Takahata et al., 1999) © 1999 IEEE.

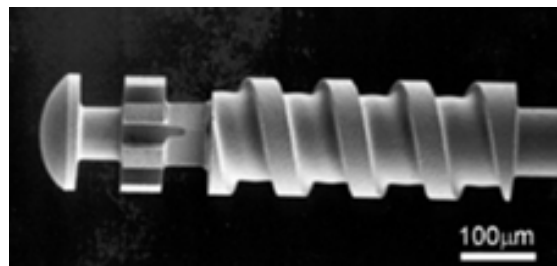


Fig. 3. A sample stainless-steel 3-D structure machined using a 5-axis  $\mu$ EDM system.

Relaxation-type resistor-capacitor ( $R$ - $C$ ) circuitry has been predominantly employed to control pulse generation/ timing in  $\mu$ EDM systems (Masuzawa & Sata, 1971). The discharge energy ( $E$ ) of a single pulse provided through this type of circuit can be expressed as:

$$E = \frac{1}{2}(C + C_p)V^2 \quad (1)$$

where  $C$  is the capacitance of the circuit,  $C_p$  is the lumped parasitic capacitance present in parallel to  $C$ , and  $V$  is the machining voltage. There is a trade-off between the smoothness of machined surfaces and machining speed, as a function of discharge energy; the greater the discharge energy, the larger the volume removed by a single pulse (i.e., faster machining) but the rougher the surfaces. To achieve stable discharge, the voltage is typically set above 60 V, up to 100 V. For finer machining,  $C$  is often set to be zero, using  $C_p$  only. Therefore, in order to minimize removal size and surface roughness, it is critical to reduce  $C_p$ , as it directly impacts the discharge energy and thus the unit removal volume by a single discharge. The machining systems are configured to achieve minimal  $C_p$  resulting from their

components (e.g., using bulk ceramics as mechanical parts). Another common type of pulse generator for conventional EDM is based on transistor (FET) switching circuitry. This type of generator can generate pulses at higher frequencies and hence remove material faster, but is in general limited in generating the short pulses required in  $\mu$ EDM. However, efforts have been made to overcome this issue (Hana et al., 2004).

Despite its excellent capability in terms of precision/ tolerance, surface quality and complex 3-D formation,  $\mu$ EDM has not achieved widespread use in product manufacturing primarily because of its productivity drawbacks. The throughput of conventional  $\mu$ EDM is inherently low because it is a serial process that uses a single electrode tip to machine and produce structures individually. Another related issue is electrode wear, which tends to degrade not only machining precision but also productivity when replacement of electrodes is necessary. Applications of the technique to product manufacturing implemented in the past fall into two types as summarized in Fig. 4. One is direct machining of end products. In this case, although the wide range of material options is provided by technique, removal volume needs to be small in order to achieve an acceptable level of production throughput. A representative example of this case is trimming of the magnetic heads. Another type of application is machining of replication tools (e.g., micro molds for injection molding).  $\mu$ EDM allows one to fabricate robust tools using hard alloys commonly used in molding dies (e.g., tool steel and super-hard alloy). The use of such tools enables volume manufacturing of replicated products at low costs; however material options in the replication processes are limited. It is evident that there is a trade-off relationship between productivity (or removal volume) and material as shown in Fig. 4.

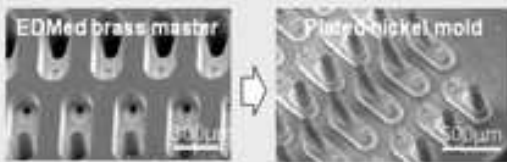
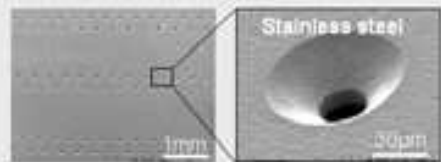
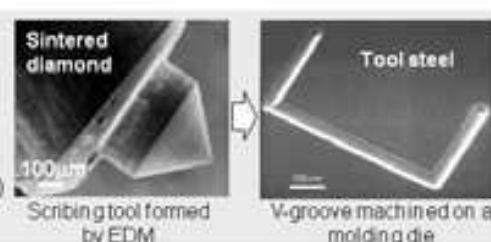
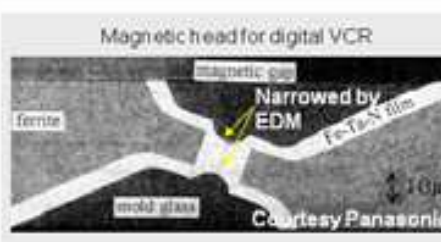
Mechanical/mold tooling		Direct machining
Inkjet printing head	 <p>EDMed brass master Plated nickel mold Ink channels (images courtesy Panasonic)</p>	 <p>Stainless steel Nozzle arrays (Hiraishi et al., 1999)</p>
V-groove mechanical patterning (Takahata & Masaki, 1999)	 <p>Sintered diamond Tool steel Scribing tool formed by EDM V-groove machined on a molding die</p>	 <p>Magnetic head for digital VCR Narrowed by EDM Courtesy Panasonic</p>
Advantage	High volume production	Broad material range
Disadvantage	Limited material range	Limited removal volume

Fig. 4. Application examples of conventional  $\mu$ EDM: Machining of mechanical tools and direct machining of end products.

One straightforward approach to addressing these constraints is to increase removal rate. This process involves increasing pulse frequency while keeping single discharge energy low, in order to achieve faster removal without sacrificing machining quality (Hana et al., 2004). However, throughput scales down as the number of structures to be machined

increases. A conceptually different approach has been investigated to convert the machining mode of  $\mu$ EDM from serial to parallel or batch. This conversion has been realized by utilizing arrays of microelectrodes to implement planar processing, as will be discussed in the next section. This approach offers opportunities to achieve not only high-throughput production, due to its high parallelism, but also compatibility with other planar microfabrication techniques based on lithography processes, which are the mainstream of MEMS manufacturing. The latter feature potentially enables the integration of  $\mu$ EDM with standard MEMS technologies, realizing heterogeneous microstructures and devices with unique functionalities and performance.

### 3. Advanced $\mu$ EDM enabled by photolithography and MEMS

This section discusses new types of  $\mu$ EDM techniques developed to enable batch micromachining and manufacturing for microdevices and their components. It has been demonstrated that the use of microelectrode arrays is a very effective route to reach this goal. This approach has been extended to a technique that leverages MEMS actuators to further advance the capability of the technique. Details follow below.

#### 3.1 Batch-mode $\mu$ EDM

The concept of parallel/ batch  $\mu$ EDM processing enabled by electrode arrays is illustrated in Fig. 5. Photolithographic methods offer various paths to the fabrication of such arrays with arbitrary patterns on a substrate. The following are the major advantages of using lithographically fabricated electrodes over conventional single electrodes.

- Parallel machining of multiple structures for high-throughput production.
- Photo-patterned electrodes are precisely arranged on the substrate and have high structural uniformity across the arrays, offering high precision and uniformity in the machined products.
- Batch production of electrode components with high volume and low cost.
- One electrode only is used for machining one structure, in contrast to the conventional serial-processing method (i.e., one electrode for all structures), minimizing consumption/ wear per electrode, and machining errors.

A common approach to electrode fabrication is to use a patterned photoresist layer as a mold for electroplating of electrode material. To deal with machining that involves deep or 3-D structures, the electrodes are often required to be high-aspect-ratio microstructures (HARMST). The process that provides HARMST with the highest precision among other techniques is deep X-ray lithography, known as LIGA (German acronym for lithography, electroforming and molding). A group from Germany and Switzerland first demonstrated  $\mu$ EDM using LIGA electrodes of electroplated copper with arbitrary patterns (Ehrfeld et al., 1996). In this application, the final step of molding is omitted, i.e., the electroplated structures are the end product, serving as the  $\mu$ EDM electrodes. This approach was advanced in the US, where LIGA fabricated electrode arrays were successfully utilized to demonstrate parallel machining of microstructures (Takahata et al., 2000; Takahata & Gianchandani, 2002).

A LIGA process used for electrode fabrication is shown in Fig. 6. This process, developed at the University of Wisconsin-Madison, utilizes thick, solid polymethylmethacrylate (PMMA) sheet as the photoresist for synchrotron X-ray lithography (Guckel, 1998). One important

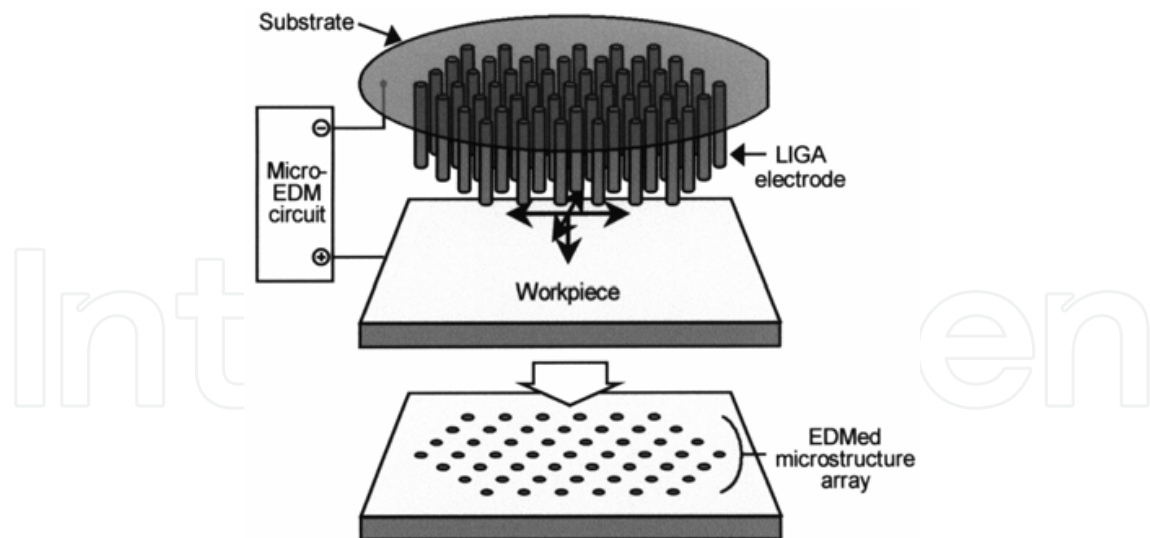


Fig. 5. Concept of batch-mode  $\mu$ EDM (Takahata & Gianchandani, 2002) © 2002 IEEE.

feature of  $\mu$ EDM that makes the use of this type of HARMST electrode feasible is that the process does not produce contact forces to the electrodes that lead to peeling of the structures from the substrate. Figure 7a shows an example of a  $20 \times 20$  array of HARMST electrodes of electroplated copper with  $20\text{-}\mu\text{m}$  diameter,  $60\text{-}\mu\text{m}$  pitch, and  $300\text{-}\mu\text{m}$  structural height. For  $\mu$ EDM, the electrode substrate is mounted on the X-Y stage of a  $\mu$ EDM machine, and a workpiece held on the vertical Z stage of the machine is advanced into the arrays along the axial direction of the electrodes to perform batch-mode machining. Results obtained with stainless-steel samples are shown in Figs. 7b and 7c. Figure 8 shows a honeycomb structure fabricated in  $125\text{-}\mu\text{m}$ -thick graphite sheet by using arrayed electrodes with hexagonal pattern shape. Since graphite has high thermal conductivity, such structures may be suitable for heat exchange applications. In conventional  $\mu$ EDM, a

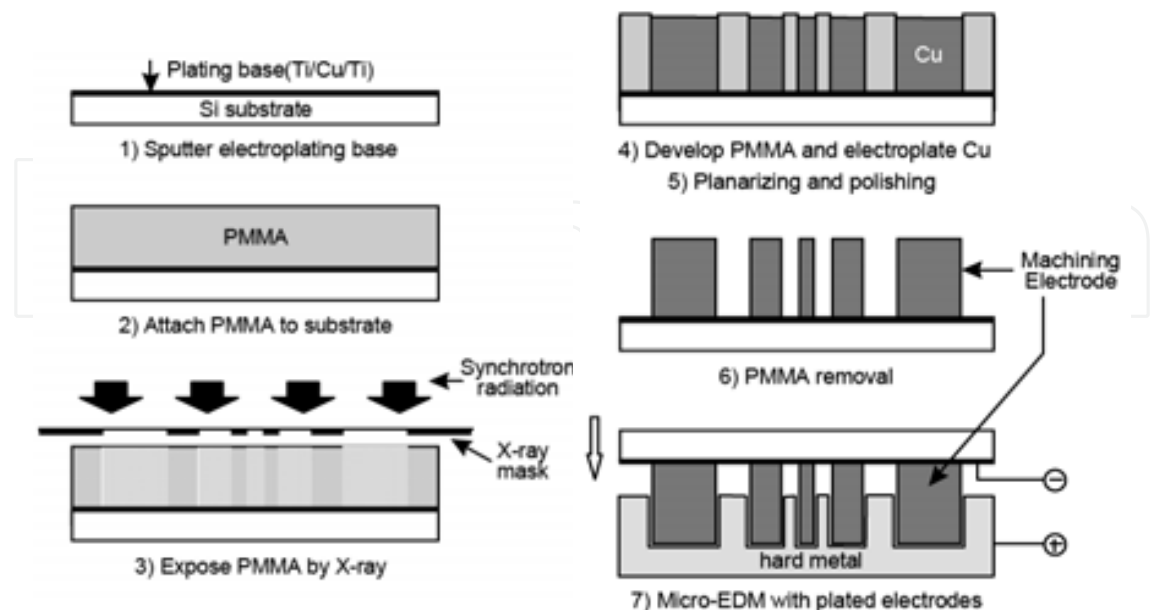


Fig. 6. A LIGA process for electrode fabrication, and subsequent  $\mu$ EDM using the electrodes (Takahata et al., 1999) © 1999 IEEE.

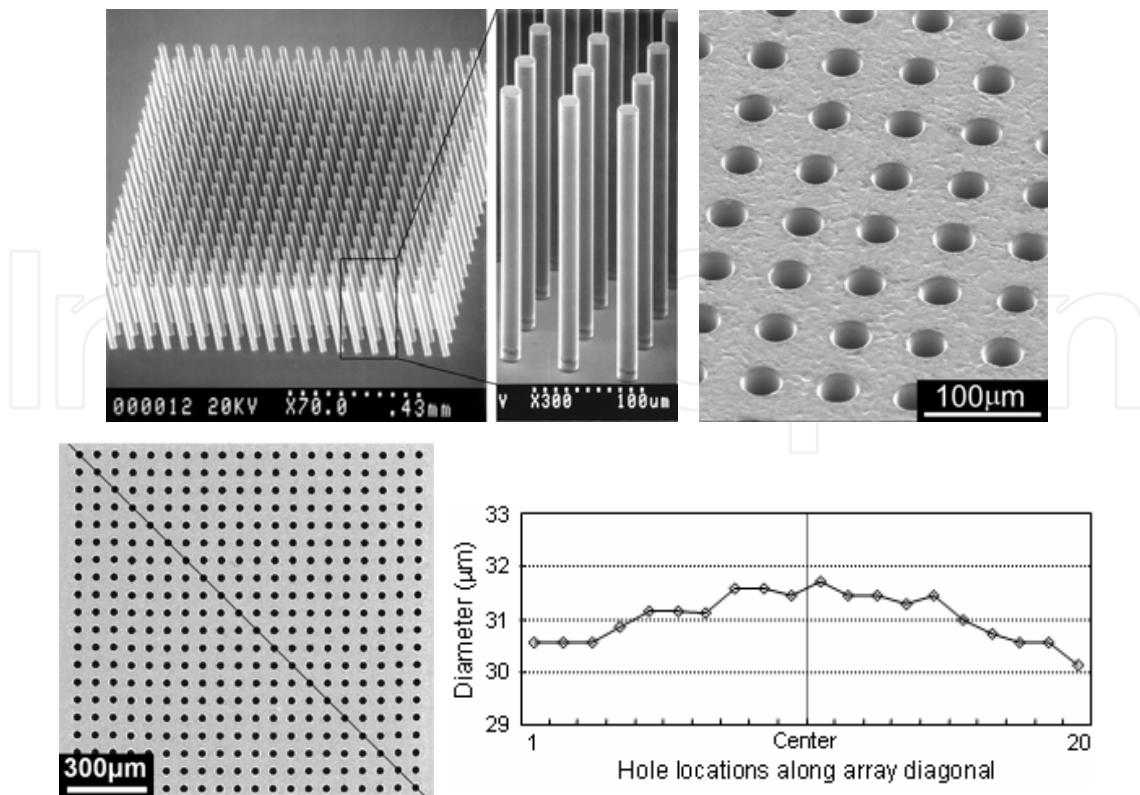


Fig. 7. (a: upper left) A 20×20 array of LIGA fabricated copper electrodes; (b: upper right) through-holes batch machined in 50-μm-thick stainless steel using the array; (c: lower) a top-view image of the machined hole array, and measured variation of hole diameter along the array diagonal shown in the image (Takahata & Gianchandani, 2002) © 2002 IEEE.

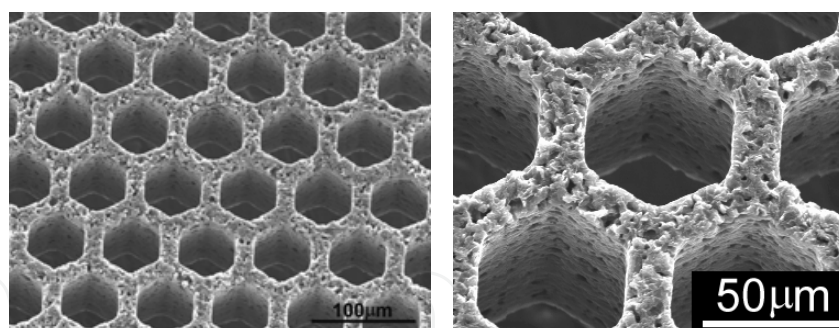


Fig. 8. Graphite honeycomb microstructures (hexagonal pitch of 70 μm and wall thickness of 16 μm) formed by batch-mode μEDM (Takahata & Gianchandani, 2002) © 2002 IEEE.

cylindrical electrode is rotated during the machining process in order to increase uniformity and prevent local welding to the workpiece. This rotation is clearly not possible when using arrayed electrodes. Instead, the electrodes are placed on a vibrator that dithers them along the axis of approach.

Figure 9 shows microchannels fabricated by the sequential application of arrayed electrodes of three different shapes, each of which contributes to a structural "layer". The layer-to-layer alignment resolution of 100 nm is afforded by the precision of workpiece movement in μEDM and the tight dimensional tolerance of LIGA. Note that each nozzle in the figure has a 40° taper at the top. This was created by a scrolling motion of the electrode array. The

result demonstrates that the combination of lithographically fabricated electrodes and  $\mu$ EDM can be used to create complex multi-layer structures in bulk metals.

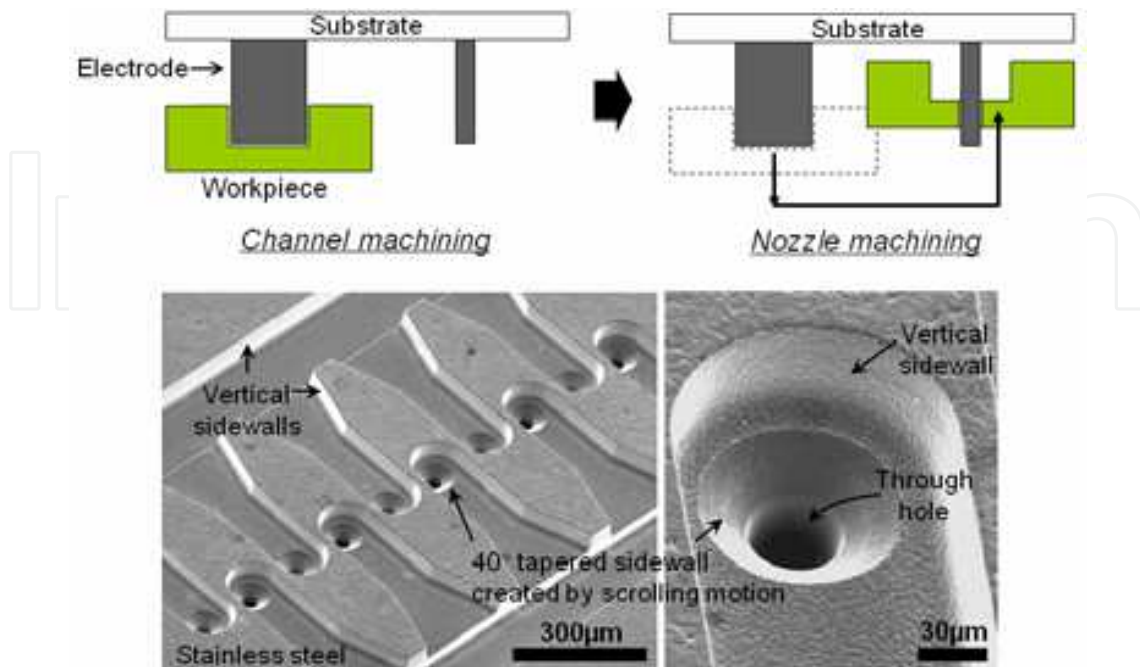


Fig. 9. (a: upper) Sequential application of electrodes formed on a substrate; (b: lower) microchannels fabricated by the technique (Takahata & Gianchandani, 2001) © 2001 IEEE.

Although the presence of multiple electrodes can increase spatial parallelism, temporal parallelism is not achieved if a single pulse discharge circuit is used, because only one electrode fires at a time. In this case, as the number of electrodes in the array increases, the pulse frequency at each of the electrodes drops. This means that the removal rate at individual electrodes will decrease, thus the throughput does not scale up as the number of electrodes increases. Further gains in throughput can be achieved by partitioning the electrode array into segments, each of which is controlled by a separate pulse generation circuit (Takahata & Gianchandani, 2002). The use of monolithically partitioned electrode arrays coupled with multiple  $R$ - $C$  circuits through thin film interconnect patterned on their substrate demonstrated parallel discharging at the arrays, maximizing pulse frequencies at individual electrodes for accelerated processing. Figure 10 shows LIGA electrode arrays with interconnect to individual electrodes as well as batch-produced micro gears cut from 70- $\mu$ m-thick WC-Co super-hard alloy sheet using the arrays. This experiment showed improvement in throughput by  $>100\times$  compared to that in traditional serial  $\mu$ EDM. This arrangement permits on-chip parasitic capacitance present in each of the partitioned electrodes to be used as a capacitor of the  $R$ - $C$  circuit, which is highly amenable to large-sized arrays because all the pulse control circuit elements can be integrated.

The machining process produces debris containing the particles removed from the workpiece and carbon residues produced by pyrolysis of dielectric EDM oil during the process. Debris removal from the machining region is critical to perform well-controlled  $\mu$ EDM, as its presence in the region tends to cause enlarged discharge gaps and tolerances as well as irregular continuous arcs, which thermally damage both the electrode and the workpiece. In traditional  $\mu$ EDM using a single cylindrical electrode, the rotation of the

electrode and open space around it promote the dispersion of debris from the machining region. In batch-mode  $\mu$ EDM using planar electrodes, however, removal of debris becomes a challenging issue as the tool movement is limited to the dither motion. In addition, a large planar form of the tool limits the flow of EDM fluid and options for flushing. It has been reported that a two-step hydrodynamic debris removal technique can address this issue effectively, resulting in improved surface and edge finish, machining time, and tool wear over the method that uses standard vertical dither flushing (Fig. 11).

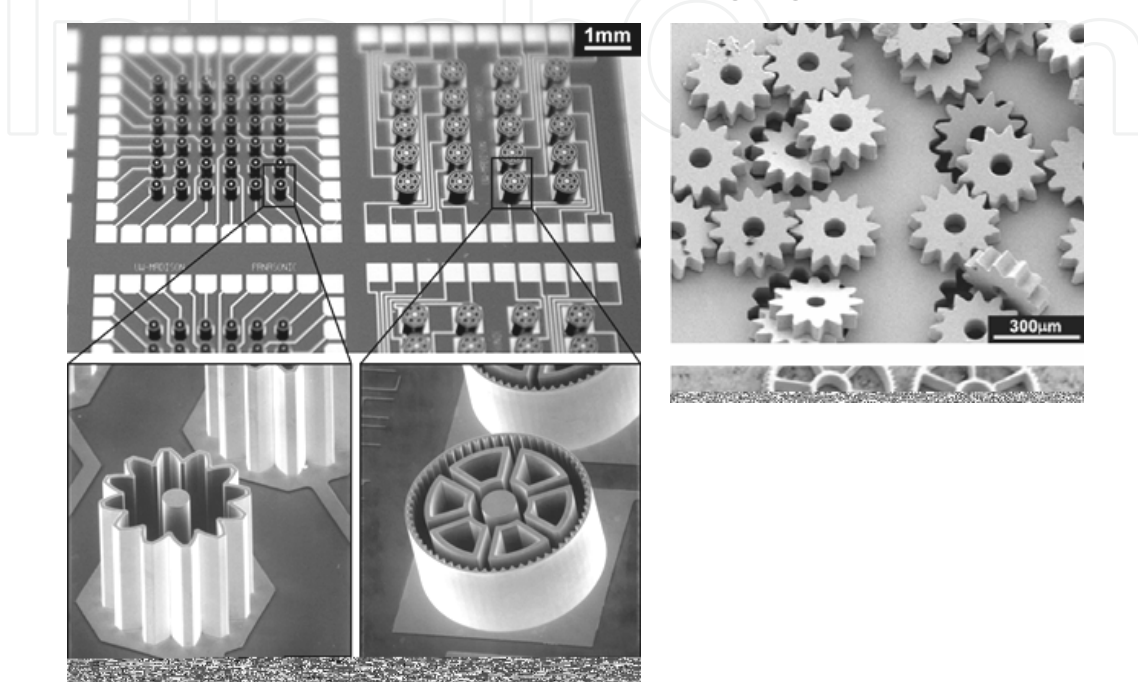


Fig. 10. (a: left) Partitioned copper electrode arrays with interconnect; (b: right) super-hard alloy gears batch produced using the arrays (Takahata & Gianchandani, 2002) © 2002 IEEE.

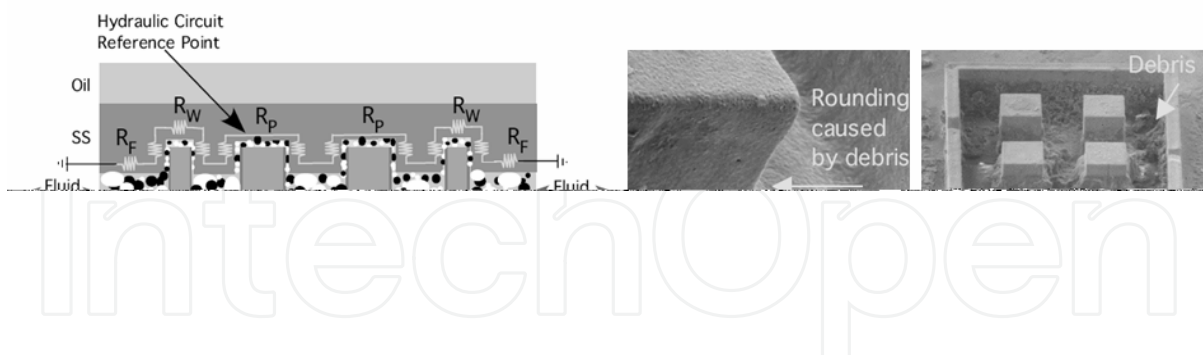


Fig. 11. Cross-section of hydraulic resistance circuit and machined result with (top) standard dither flushing and (bottom) hydrodynamic flushing (Richardson et al., 2006) © 2006 IEEE.

### 3.2 MEMS-based $\mu$ EDM

Although the batch-mode method discussed above demonstrated improved throughputs, it is still limited in the machinable area due to the available size of the substrate holding the arrays. This implementation requires a high-cost  $\mu$ EDM system and an NC stage of the system to advance planar electrode arrays into the workpiece, which also limits the substrate size to be compatible with the stage. Toward  $\mu$ EDM of large-area samples (e.g., shape memory alloy foil for microactuator fabrication and hard-alloy plates to form microstructured molding dies), a new technique called M<sup>3</sup>EDM (MEMS-based micro-EDM) has been developed. This  $\mu$ EDM method uses micromachined actuators with movable planar electrodes that are fabricated directly on the workpiece material using lithography techniques and actuated to perform machining. The actuation leverages electrostatic forces generated by a machining voltage applied between the electrode and the workpiece (Alla Chaitanya & Takahata, 2008a). This approach offers an opportunity to eliminate NC machines from the process, achieving high scalability to very large areas for high-throughput, low-cost micromanufacturing.

Figure 12 illustrates the mechanical and electrical behaviors of the electrode device in the machining process. The planar electrodes are microfabricated so that they are suspended by the anchors through tethers above the surfaces of the conductive workpiece with a relatively large gap. The application of machining voltage produces electrostatic forces that drive the electrodes towards the workpiece. With properly designed structures at a selected voltage, the phenomenon known as “pull-in” takes place, when the restoring spring force through the tethers can no longer balance the electrostatic force as the gap spacing decreases. This results in a breakdown and produces a pulse current due to a discharge from the capacitors (external capacitor  $C$  and built-in capacitor  $C_b$  in Fig. 12) that removes the material at the local spot. The discharge lowers the voltage between the electrode and the workpiece, releasing the electrode. Simultaneously, the capacitors are charged through the resistor, restoring the voltage at the gap and inducing the electrostatic actuation again. This sequence of pull-in and release of the electrode is used to achieve self-regulated generation of discharge pulses that etch the material. This approach that uses electrostatic actuation is suitable for selected electrode structures and applications requiring relatively shallow machining due to the limitation of its actuation range. An M<sup>3</sup>EDM method that uses downflow of dielectric EDM fluid for electrode actuation has been demonstrated to overcome this limitation in the electrostatic actuation method (Alla Chaitanya & Takahata, 2008b).

The fabrication of movable electrodes on workpieces was implemented by a combination of film lamination, photolithography, and wet etching of 18- $\mu$ m-thick copper foil used as the structural material of the electrode device. Figure 13 shows the electrode devices formed on a piece of dry-film photoresist that can be laminated on the target workpiece. The photoresist serves as the sacrificial layer, which is dissolved to release the electrode structures. This method, where electrodes are supplied with laminatable film, is potentially applicable to samples that have non-planar surfaces to be machined, or those whose sizes are incompatible with photolithography tools, making direct fabrication of the devices on them difficult. Figure 14a shows another electrode fabrication process that uses liquid photoresist. This process was developed to incorporate arbitrary features on the backside of

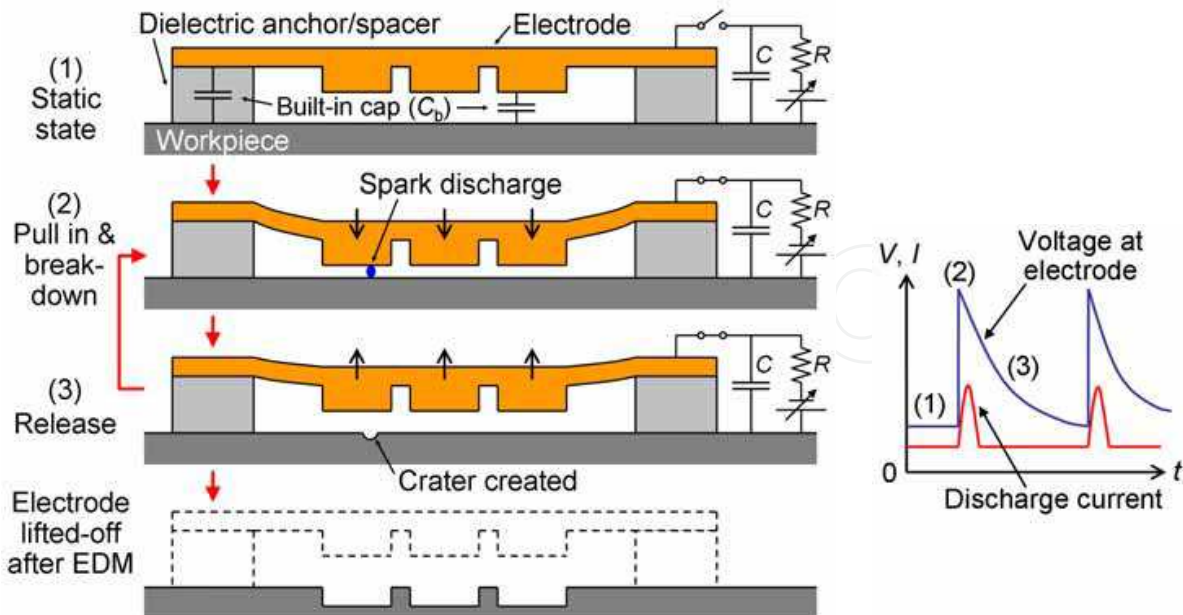


Fig. 12. (a: left) Cross-sectional view of M<sup>3</sup>EDM and its process steps; (b: right) dynamic behavior of discharge voltage and current corresponding to the steps (Alla Chaitanya & Takahata, 2008a) © 2008 IEEE.

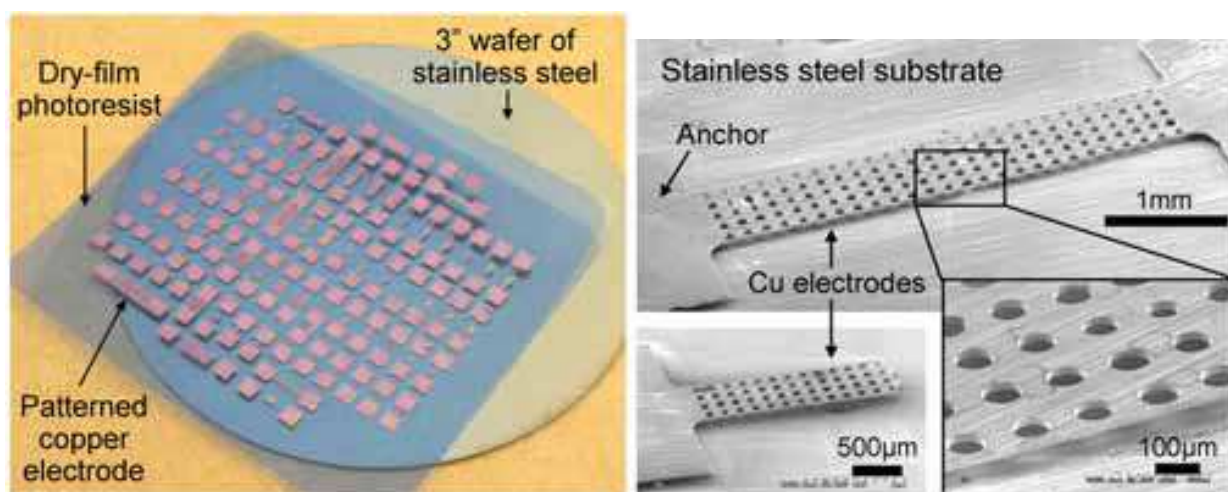


Fig. 13. (a: left) A 6×6 cm<sup>2</sup> piece of sacrificial dry-film photoresist with patterned electrode devices; (b: right) examples of fabricated electrode devices with fixed-fixed and cantilever configurations (Alla Chaitanya & Takahata, 2008b) © 2008 IOP Publishing Ltd.

the planar electrodes for  $\mu$ EDM of custom patterns. The fabricated electrode arrays shown in Fig. 14b were designed to have a crab-leg configuration to support planar electrodes with larger areas. Pattern transfer to stainless-steel wafers (which served as the workpieces in this experiment) was successfully demonstrated (Fig. 14c). The development of M<sup>3</sup>EDM is currently in progress toward enabling high-precision, cost-effective batch  $\mu$ EDM for large-area micromachining of bulk metals and alloys.

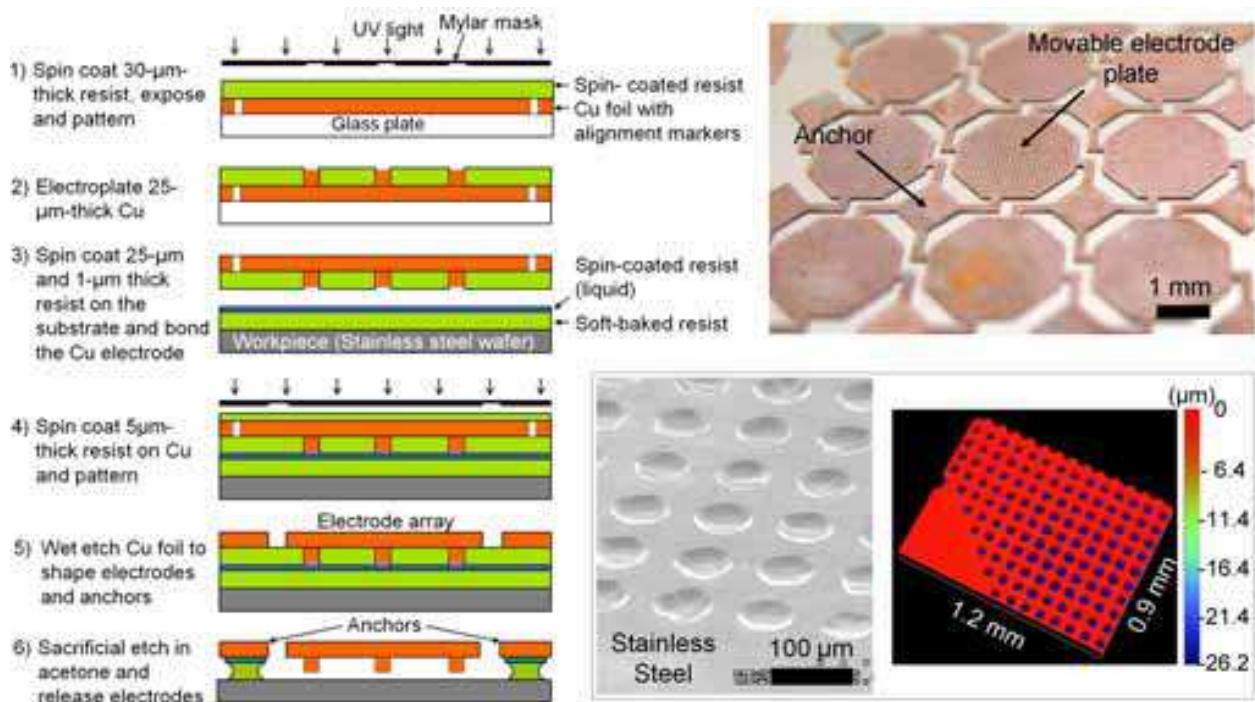


Fig. 14. (a: left) Fabrication process flow for double-layer electrode devices; (b: upper right) a fabricated array of planar electrodes that hold arrayed microstructures on the backside of the electrodes; (c: lower right) batch-machined structures created in stainless steel (Alla Chaitanya & Takahata, 2009) © 2009 IEEE.

#### 4. Application

The application of  $\mu\text{EDM}$  to MEMS and micro-scale devices has been primarily driven by demand for use of bulk metals and alloys with unique performance that are difficult to be micromachined using lithography and etching processes. The most common application involves micromachining of mechanical components of the devices. For example, a rotor and bearing parts were machined using  $\mu\text{EDM}$  and assembled to construct a micro air turbine (Masaki et al, 1990). Another micro turbine with a more complex design was reported in (Peirs et al., 2002), where the components were fabricated by a combination of  $\mu\text{EDM}$  and mechanical machining. Although stainless steel was the main structural material in these particular devices, the technique allows one to select harder alloys to construct devices in order to achieve more robust mechanical systems; an example is described in Subsection 4.1. An implantable device called a stent is presented in Subsection 4.2 as another example of mechanical devices fabricated by  $\mu\text{EDM}$ . The technique has been used for bulk micromachining of heavily doped single crystal silicon (Reynaerts et al., 1997; Heeren et al., 1997), and it has been integrated with lithography processes to construct an inertial sensor (Reynaerts et al., 2000). Needle-shaped HARMST neural electrode arrays have been fabricated from highly doped silicon using a combination of wire  $\mu\text{EDM}$  and isotropic wet etching (Tathireddy et al., 2009).  $\mu\text{EDM}$  has also been leveraged to produce components from permanent magnet and ferromagnetic material that are incorporated in electromagnetic MEMS sensors and actuators (Grimes et al., 2001; Fischer et al., 2001). In addition to the machining (and assembly) of mechanical/ magnetic components mentioned above, various efforts have utilized  $\mu\text{EDM}$  to construct devices with electrical

functionalities. A common need for this application is to integrate dielectric materials with  $\mu$ EDM structures to create electrical partitions and circuits in the devices. This is a challenging task, because  $\mu$ EDM by itself does not allow electrical isolation, since all the mechanically connected features are also all electrically connected. This issue has been addressed through different fabrication approaches, described in the development of the devices presented in Subsections 4.3 to 4.6, i.e., antenna stent, scanning micro Kelvin probe, electromagnetic flow sensor, and capacitive pressure sensor.

#### 4.1 Self-propelled micromachine

A chain-type, self-propelled micromachine has been developed for the maintenance of power plants, where chained micromachines perform the inspection of the outer surfaces of tube banks (Takeda et al., 2000). The traveling device of the micromachine uses a micro reducer based on a paradox planetary gear system to achieve high torque with a micromotor, as well as magnetic wheels to achieve strong traction (Fig. 15). The gears and other mechanical components were fabricated by  $\mu$ EDM of hard alloys such as high-carbon tool steel and WC-Ni-Cr super-hard alloy. The fabrication precision in  $\mu$ EDM of the gear components was reported to be within 0.4 %, with standard deviation of 0.127. Here the machining error is largely associated with the wear of electrodes. The developed micro reducer with as-machined planetary gears (without any surface coating) and oil-lubricated rolling bearing was observed to sustain sufficient performance after  $5 \times 10^6$  rotations (Takeuchi et al., 2000). These results demonstrate that  $\mu$ EDM is a practical fabrication technique for realizing high-precision mechanical systems with high robustness. A major drawback to the manufacturing of such systems is the need for assembly of the machined components. An example addressing this issue was reported in (Sun et al., 1996), where a micro turbine device with rotor, bearing, and base components was constructed in a pre-assembly manner using a process based on  $\mu$ EDM and micro ultrasonic machining.

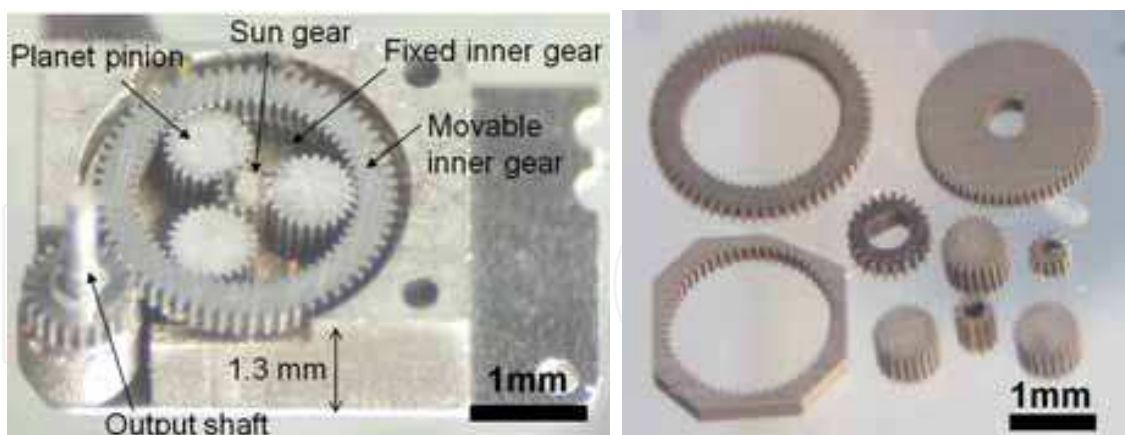


Fig. 15. (a: left) Gear reduction system developed for a self-propelled micromachine; (b: right) WC-Ni-Cr super-hard alloy gear components of the system produced by  $\mu$ EDM; most of the gears have a module number of 0.03 (images courtesy of Dr. Narito Shibaiki).

#### 4.2 Micromechanical stents

Stents are mechanical devices that are chronically implanted into arteries in order to physically expand and scaffold blood vessels that have been narrowed by plaque accumulation. The vast majority of stents are manufactured by laser machining of metal

tubes made of biocompatible stainless steel or shape memory alloy, creating mesh-like walls that allow the tube to be expanded radially upon the inflation of an angioplasty balloon (Kathuria, 1998). The use of  $\mu$ EDM is another option for cutting metal microstructures. It has been shown that tubular stents can be fabricated from planar stainless-steel foil using  $\mu$ EDM (Takahata & Gianchandani, 2004a). The planar design of the stent also permits the use of the batch machining method discussed in Subsection 3.1. The planar pattern has two longitudinal side-beams, connected transversely by expandable cross-bands, each of which contains identical involute loops (Fig. 16a). In a manner identical to that used with commercial stents, the stent was deployed by inflating an angioplasty balloon threaded through the planar structure such that the transverse bands alternated above and below it; the structure was plastically deformed into a cylinder shape when deployment was completed. Figure 16b shows an expanded stent with the balloon removed. Mechanical tests indicated that the developed stent had almost the same radial strength as a commercial stent (Guidant Multilink Tetra™) tested for comparison, even though the developed stent had a wall thickness (of 50  $\mu$ m) that was approximately one-half that of the commercial stent. The radial stiffness was similar when the loading was applied at two extreme orientations, i.e., perpendicular to the original plane of the pre-expansion planar microstructure and parallel to the plane.

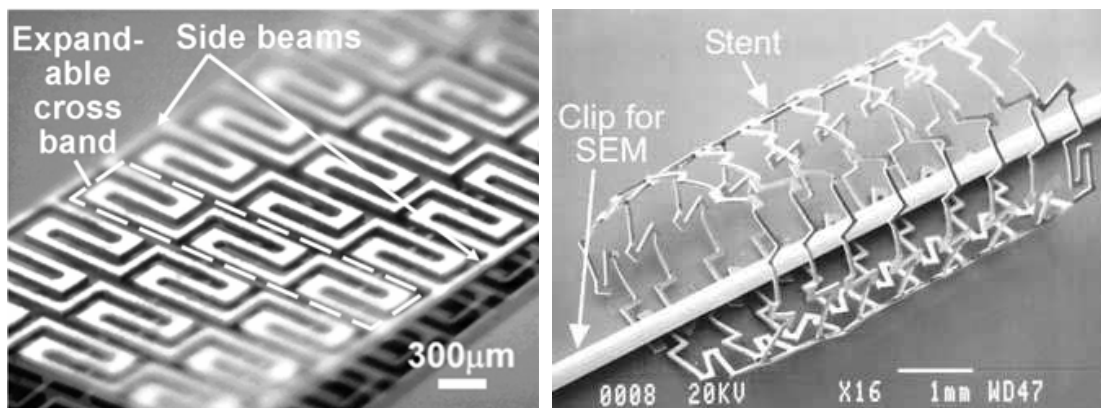


Fig. 16. (a: left) A 7-mm-long planar stent sample as cut by  $\mu$ EDM from 50- $\mu$ m-thick stainless-steel foil; (b: right) an expanded state of the planar structure with diameter of 2.65 mm (Takahata & Gianchandani, 2004a) © 2004 IEEE.

#### 4.3 Antenna stents

Following stent implantation, re-narrowing (restenosis) of the artery often occurs. To determine the status, patients are required to have an X-ray angiograph, potentially multiple times. Since this is an invasive procedure involving insertion of a catheter to inject contrast dye, it cannot be performed frequently. Wireless monitoring of cardiac parameters such as blood pressure and flow can provide advance notice of restenosis. Toward this end, the planar approach for stent fabrication described above was leveraged to develop a method that automatically transforms the electrical characteristics of a stent during balloon angioplasty, allowing the stent to be a helical-shaped antenna (stentenna) (Takahata et al., 2006). The planar design of the stent enables the use of lithography-based micromachining techniques for direct fabrication of sensors on the stent as well as the integration of separately fabricated microsensor chips. The planar device has a series of involute cross-

bands similar to those used in the mechanical stent described in Subsection 4.2, but designed to form dual inductors when the device is expanded to a cylindrical shape. Two micromachined capacitive pressure sensor chips were bonded to the planar stent structure and connected across the common line and the inductors, implementing a dual inductor-capacitor ( $L$ - $C$ ) tank configuration (Fig. 17a). In other words, integration of dielectric material (used to establish the sensing capacitor) with  $\mu$ EDM structures was implemented by a hybrid method, i.e., individual component assembly and packaging in this fabrication. The resonant frequency of the tank, which depends on local pressure or flow rate, was wirelessly interrogated through an external antenna magnetically coupled to the stentenna. The device was coated with Parylene-C™ for electrical protection while granting it biocompatibility. The stentenna was deployed inside a mock artery using a standard angioplasty balloon (Fig. 17a), resulting in a helical shape with inductance of  $\sim 110$  nH. Wireless tests in a fluidic set-up showed that the device exhibited a frequency response of 9-31 KHz per mL/ min. in the flow range over 370 mL/ min (Fig. 17b).

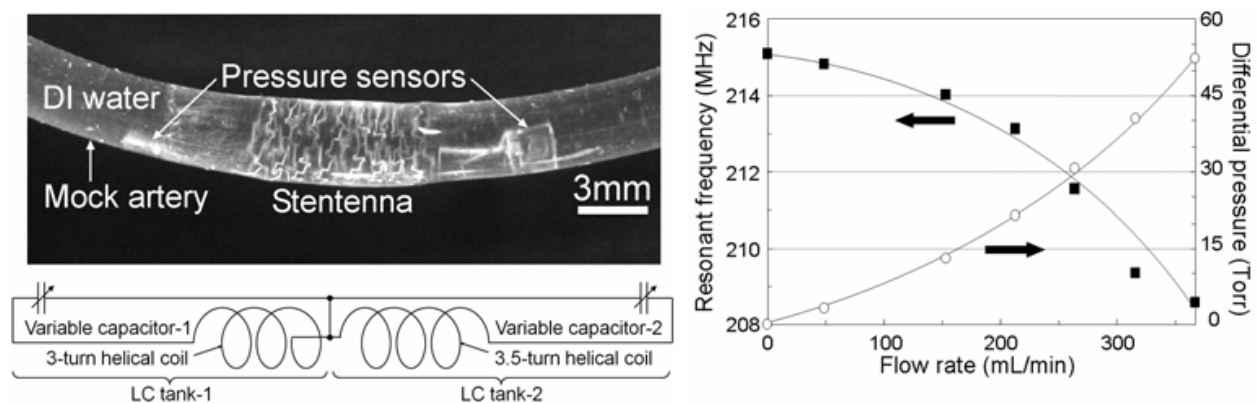


Fig. 17. (a: left) A deployed stentenna with pressure sensors and an equivalent electrical model of the deployed device; (b: right) measured resonant frequency of the stentenna as a function of flow rate (Takahata et al., 2006) © 2006 IEEE.

#### 4.4 Microactuator-integrated scanning Kelvin probe

Kelvin probes are used to measure the contact potential difference (CPD) between materials, which cannot be measured directly using a voltmeter. One of the major applications is the characterization of solid-state devices. A probe is placed above the surface of a sample in close proximity, and an AC current is generated by dithering the gap where a CPD-induced charge is built up. The bias voltage that nulls the current indirectly determines the CPD. The micromachined probe developed by  $\mu$ EDM includes an actuator that provides the axial dither motion and a lead transfer beam for the probe (Fig. 18a). An electrothermal bent-beam actuator (Que et al., 2001) provides the dither motion with amplitude in the 10- $\mu$ m range with drive voltages of a few volts. An isolation plug mechanically couples the probe to the actuator while electrically and thermally decoupling them from each other. A large width of isolation was desired to minimize the capacitive feedthrough of the drive signal as well as the thermal noise from the actuator. Monolithic integration of dielectric components (isolation plug) was achieved by the modified  $\mu$ EDM process depicted in Fig. 18b, which used a commercially available amorphous-metal foil (MetGlas 2826MB) as the conductive

material for device fabrication. The fabricated device was used for non-contact sensing of the pH of liquid inside microfluidic channels. The developed fabrication approach can potentially be applied to other devices that require mechanical structures and electrical circuits to be integrated in a monolithic manner. Further development may enable high-throughput production using batch-mode  $\mu$ EDM.

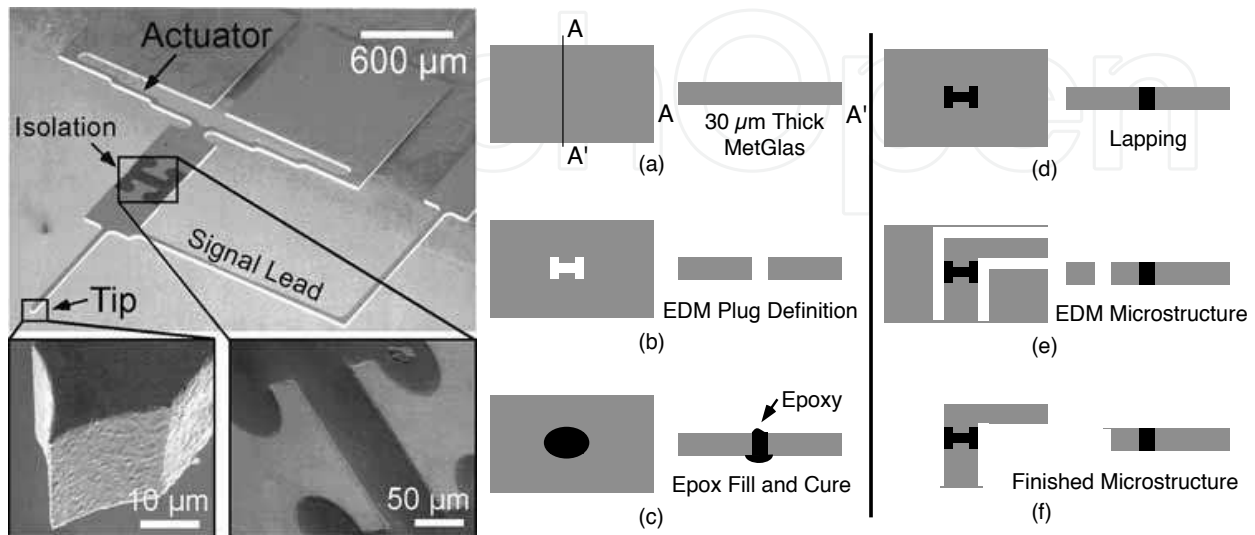


Fig. 18. (a: left) A fabricated Kelvin-probe device bonded to a glass substrate; (b: right)  $\mu$ EDM-based fabrication process for the device (Chu et al., 2005) © 2005 IEEE.

#### 4.5 Intraluminal cuff for electromagnetic flow sensing

The planar-to-cylindrical reshaping technique used in stent fabrication has been applied to the development of an intraluminal ring cuff for electromagnetic (EM) sensing of flow (Takahata & Gianchandani, 2004b). EM detection offers several attractive features, such as a direct and linear relationship between output and flow, less dependence on cross-sectional flow profile, and mechanical robustness as there are no moving parts used (Yoon et al., 2000). EM flow sensors typically have two electrodes located on inner walls of the fluid channel. In the presence of a magnetic field, a voltage proportional to the flow velocity develops between the electrodes. The planar design of the ring cuff consists of a pair of meander bands comprising 50- $\mu$ m-wide beams, electrode plates, and two dielectric links that mechanically tie the bands but electrically insulate them from each other (Fig. 19a). This pattern was created by  $\mu$ EDM in 50- $\mu$ m-thick stainless-steel foil, and then all the surfaces except the front-side planes of the electrodes were coated with an insulating layer. (Without this layer, spatial averaging would reduce the voltage.) The dielectric links (of epoxy in this case) were created by a fabrication process similar to that used for the isolation plug in the Kelvin-probe device shown in Fig. 18b. The planar structure was mounted on a deflated angioplasty balloon so that one of the bands was located above the balloon and the other was below it, which allowed the structure to assume a ring shape when the balloon was inflated. In a wired set-up (Fig. 19b), the device, expanded inside a 3-mm i.d. silicon tube, showed a response that linearly and symmetrically increased or decreased depending on the orientation of an externally applied magnetic field (Fig. 19c). Signal reading for this device was also extended to a wireless implementation using the stentenna (Takahata et al., 2006).

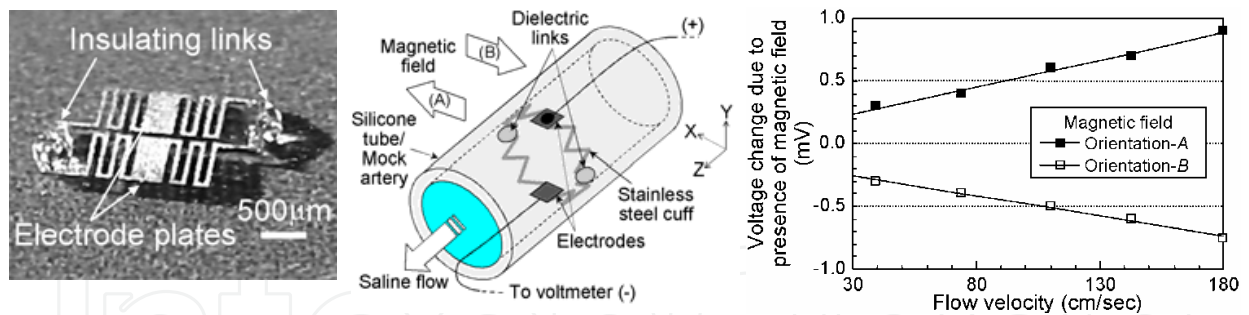


Fig. 19. (a: left) A stainless-steel cuff in the planar form; (b: middle) a fluidic measurement set-up for the expanded device; (c: right) measured responses of the device with opposing magnetic fields shown in the set-up. Figures a, b, and c are, respectively, reprints of Figs. 4, 10, and 11 in (Takahata & Gianchandani, 2004b), reprinted with the permission of the Transducer Research Foundation.

#### 4.6 Cavity/Diaphragm-less capacitive pressure sensor

Micromachined capacitive pressure sensors typically use an elastic diaphragm with fixed edges and a sealed cavity between the diaphragm and the substrate below. Since this

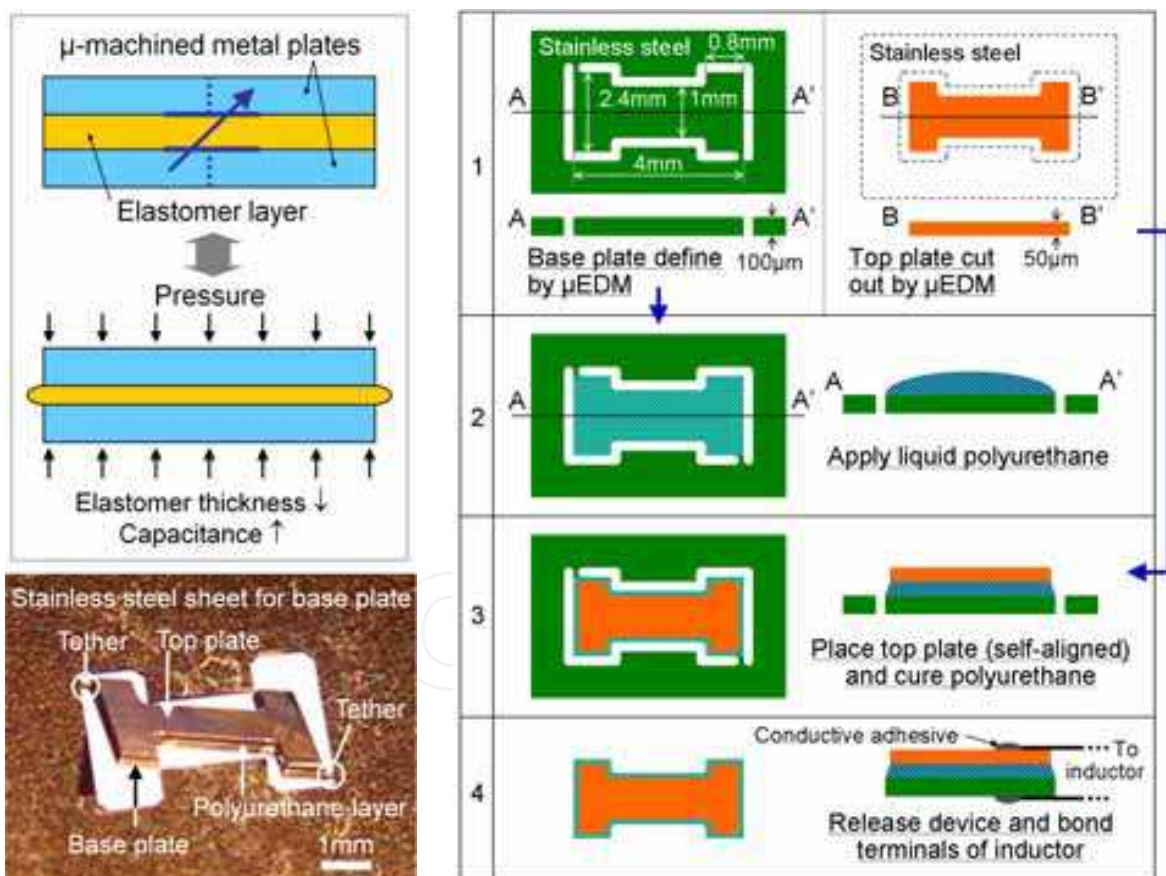


Fig. 20. (a: upper left) Cross-sectional view of the capacitive pressure sensor; (b: right) fabrication process flow; (c: lower left) a fabricated device being released from the original stainless-steel foil. Figures a, b, and c are, respectively, reprints of Figs. 1, 3, and 5a in (Takahata & Gianchandani, 2008b), reprinted with the permission of the Transducer Research Foundation.

configuration relies on the deflection of a relatively thin diaphragm against a sealed cavity, there is concern about the robustness of the diaphragm and leaks in the cavity seal in some applications. This issue has been addressed by devising a configuration consisting of two micromachined metal plates with an intermediate polymer layer, eliminating the need for diaphragms and cavities from the sensor structure (Takahata & Gianchandani, 2008a). Use of polymeric material soft enough to deform in a target pressure range allowed the thickness of the polymer, or capacitance of the parallel plate capacitor, to be dependent on the hydraulic pressure surrounding the device (Fig. 20a). The devices were constructed using micromachined stainless-steel electrodes defined by  $\mu$ EDM and a liquid-phase polyurethane that was applied and solidified between the electrodes. Figures 20b and 20c show the developed fabrication process and a fabricated device after Step 3 of the process, respectively. The integration of the liquid polyurethane with the electrode plates was achieved using a self-aligned assembly method. Pressure monitoring was demonstrated by measuring frequency shifts in the  $L$ - $C$  tank, which was fabricated by winding a copper coil on the sensor and bonding the terminals to the electrodes. Wireless operation in liquid ambient was also demonstrated (Takahata & Gianchandani, 2008b). The bulk-metal-based cavity/diaphragm-less design of the device makes it suitable for high-pressure environments. In addition, the material combination potentially permits direct use of the device in corrosive or biological environments. These features, enabled through  $\mu$ EDM-based fabrication, may contribute to reducing packaging requirements for the device in selected applications.

## 5. Conclusion

This chapter presented conventional and advanced  $\mu$ EDM technologies and discussed their application to MEMS and microdevices enabled by bulk-metal micromachining. Due to its exceptional features and versatility, this technique has great potential for making broad contributions to manufacturing not only mechanical components but also the devices and systems that equip electromechanical functionalities.  $\mu$ EDM provides unique opportunities for R&D and manufacturing of such products, as it allows leveraging of non-traditional, high-performance engineering materials with various features such as plasticity, robustness, chemical inertness, and biocompatibility that cannot be achieved through conventional MEMS fabrication processes and their compatible materials. This ability also promotes proper choice of materials that are compatible with particular environments for MEMS fabrication, potentially allowing circumvention of constraints and problems associated with packaging and broadening application opportunities for MEMS. The batch-mode machining approach enabled by the use of lithographically formed electrodes was demonstrated to be a promising means of addressing the essential drawbacks of the traditional serial technique in terms of throughput and tolerance loss, as well as making  $\mu$ EDM compatible with conventional MEMS processes based on lithography techniques. In addition, the study on  $M^3$ EDM revealed that MEMS can be utilized as means to push the limits of  $\mu$ EDM and advance the batch-machining technique. These new aspects of  $\mu$ EDM suggest that advancing the technique can be an effective way to address the constraints in the range of bulk materials available for MEMS design and manufacturing. The continued development of these new technologies will enable further breakthroughs and innovations in machining systems and MEMS manufacturing.

## 6. Acknowledgment

The M<sup>3</sup>EDM research presented in Subsection 3.2 was supported by the Natural Sciences and Engineering Research Council of Canada.

## 7. References

- Alla Chaitanya, C.R. & Takahata, K. (2008a). Micro-electro-discharge machining by MEMS actuators with planar electrodes microfabricated on the work surfaces. *Technical Digest of the 21st IEEE International Conference on Micro Electro Mechanical Systems*, pp. 375-378.
- Alla Chaitanya, C.R. & Takahata, K. (2008b). M<sup>3</sup>EDM: MEMS-enabled micro-electro-discharge machining. *Journal of Micromechanics and Microengineering*, Vol. 18, 105009 (7pp).
- Alla Chaitanya, C.R. & Takahata, K. (2009). MEMS-based batch-mode micro-electro-discharge machining using microelectrode arrays actuated by hydrodynamic force. *Technical Digest of the 22nd IEEE International Conference on Micro Electro Mechanical Systems*, pp. 705-708.
- Allen, D.M. & Lecheheb, A. (1996). Micro electro-discharge machining of ink jet nozzles: Optimum selection of material and machining parameters. *Journal of Materials Processing Technology*, Vol. 58, pp. 53-66.
- Chu, L.L.; Takahata, K.; Selvaganapathy, P.; Gianchandani, Y.B. & Shohet, J.L. (2005). A micromachined Kelvin probe with integrated actuator for microfluidic and solid-state applications. *IEEE/ASME Journal of Microelectromechanical Systems*, Vol. 14, No. 4, pp. 691-698.
- Dhanik, S. & Joshi, S.S. (2005). Modeling of a single resistance capacitance pulse discharge in micro-electro discharge machining. *Journal of Manufacturing Science and Engineering*, Vol. 127, Iss. 4, pp. 759-767.
- Ehrfeld, W.; Lehr, H.; Michel F. & Wolf, A. (1996). Micro electro discharge machining as a technology in micromachining. *Proceedings of SPIE*, Vol. 2879, pp. 332-337.
- Fischer, K.; Chaudhuri, B.; McNamara, S.; Guckel, H.; Gianchandani, Y. & Novotny, D. (2001). A latching, bistable optical fiber switch combining LIGA technology with micromachined permanent magnets. *Technical Digest of the IEEE International Conference on Solid-State Sensors and Actuators*, pp. 1340-1343.
- Grimes, C.A.; Jain, M.K.; Singh, R.S.; Cai, Q.; Mason, A.; Takahata, K. & Gianchandani, Y. (2001). Magnetoelastic microsensors for environmental monitoring. *Proceeding of the 14th IEEE International Conference on Micro Electro Mechanical Systems*, pp. 278-281.
- Guckel, H. (1998). High-aspect-ratio micromachining via deep x-ray lithography. *Proceedings of the IEEE*, Vol. 86, Iss. 8, pp. 1586-1593.
- Hana, F.; Wachi, S. & Kunieda, M. (2004). Improvement of machining characteristics of micro-EDM using transistor type isopulse generator and servo feed control. *Precision Engineering*, Vol. 28, pp. 378-385.
- Heeren, P.; Reynaerts, D.; Van Brussel, H.; Beuret, C.; Larsson, O. & Bertholds, A. (1997). Microstructuring of silicon by electro-discharge machining (EDM) - part II: Applications. *Sensors and Actuators A*, Vol. 61, Iss. 1-3, pp. 379-386.

- Hiraishi, M.; Masaki, T. & Muro, M. (1999). High-speed micro EDM of micro nozzles. *Proceeding of the Annual Meeting of the Japanese Society of Electrical Machining Engineers*, pp. 45-48.
- Ho, K.H.; Newman, S.T.; Rahimifard, S. & Allen, R.D. (2004). State of the art in wire electrical discharge machining (WEDM). *International Journal of Machine Tools and Manufacture*, Vol. 44, Iss. 12-13, pp. 1247-1259.
- Honma, Y.; Takahashi, K. & Muro, M. (1999). Micro-machining of magnetic metal film using electro-discharge technique. *Advances in Information Storage Systems*, Vol. 10, pp. 383-399.
- Kathuria, Y.P. (1998). Laser microprocessing of stent for medical therapy. *Proceedings of the IEEE International Symposium on Micromechatronics and Human Science*, pp. 111-114.
- Laermer, F. & Urban, A. (2005). Milestones in deep reactive ion etching. *Digest of technical Papers, the 13th International Conference on Solid-State Sensors, Actuators and Microsystems*, Vol. 2, pp. 1118-1121.
- Masaki, T.; Kawata, K. & Masuzawa, T. (1990). Micro electro-discharge machining and its applications. *Proceedings of the IEEE International Workshop on Micro Electro Mechanical Systems*, pp. 21-26.
- Masuzawa, T.; Fujino, M.; Kobayashi, K.; Suzuki, T. & Kinoshita, N. (1985). Wire electro-discharge grinding for micro-machining. *Annals of the CIRP*, Vol. 34, pp. 431-434.
- Masuzawa, T. & Sata, T. (1971). The occurring mechanism of the continuous arc in micro-energy EDM by RC circuit. *Journal of the Japan Society of Electrical Machining Engineers*, Vol. 5, No. 9, pp. 35-52.
- Peirs, J.; Reynaerts, D.; Verplaetsen, F.; Poesen, M. & Renier, P. (2002). A microturbine made by micro-electro-discharge machining. *Proceedings of the 16th European Conference on Solid-State Transducers*, pp. 790-793.
- Que, L.; Park, J.S. & Gianchandani, Y.B. (2001). Bent-beam electro-thermal actuators-I: Single beam and cascaded devices. *IEEE/ASME Journal of Microelectromechanical Systems*, Vol. 10, No. 2, pp. 247-254.
- Reynaerts, D.; Heeren, P. & Van Brussel, H. (1997). Microstructuring of silicon by electro-discharge machining (EDM) - part I: Theory. *Sensors and Actuators A*, Vol. 60, Iss. 1-3, pp. 212-218.
- Reynaerts, D.; Meeusen, W.; Song, X.; Van Brussel, H.; Reyntjens, S.; De Bruyker, D. & Puers, R. (2000). Integrating electro-discharge machining and photolithography: Work in progress. *Journal of Micromechanics and Microengineering*, Vol. 10, pp. 189-195.
- Richardson, M.T.; Gianchandani, Y.B. & Skala, D.S. (2006). A parametric study of dimensional tolerance and hydrodynamic debris removal in micro-electro-discharge machining. *Technical Digest of the 19th IEEE International Conference on Micro Electro Mechanical Systems*, pp. 314-317.
- Sato, K.; Shikida, M.; Matsushima, Y.; Yamashiro, T.; Asaumi, K.; Iriye, Y. & Yamamoto, M. (1998). Characterization of orientation dependent etching properties of single crystal silicon: Effects of KOH concentration. *Sensors and Actuators A*, Vol. 64, No. 1, pp. 87-93.
- Sun, X.; Masuzawa, T. & Fujino, M. (1996). Micro ultrasonic machining and its applications in MEMS. *Sensors and Actuators A*, Vol. 57, Iss. 2, pp. 159-164.

- Takahata, K.; Aoki, S. & Sato, T. (1997). Fine surface finishing method for 3-dimensional micro structures. *IEICE Transactions on Electronics*, Vol. E80-C, No. 2, pp. 291-296.
- Takahata, K. & Gianchandani, Y.B. (2001). Batch mode micro-EDM for high-density and high-throughput micromachining. *Proceedings of the 14th IEEE International Conference on Micro Electro Mechanical Systems*, pp. 72-75.
- Takahata, K. & Gianchandani, Y.B. (2002). Batch mode micro-electro-discharge machining. *IEEE/ASME Journal of Microelectromechanical Systems*, Vol. 11, No. 2, pp. 102-110.
- Takahata, K. & Gianchandani, Y.B. (2004a). A planar approach for manufacturing cardiac stents: Design, fabrication, and mechanical evaluation. *IEEE/ASME Journal of Microelectromechanical. Systems*, Vol. 13, No. 6, pp. 933-939.
- Takahata, K. & Gianchandani, Y.B. (2004b). A micromachined stainless steel cuff for electromagnetic measurement of flow in blood vessels. *Proceeding of Solid-State Sensor, Actuator and Microsystems Workshop*, pp. 290-293.
- Takahata, K. & Gianchandani, Y.B. (2007). Bulk-metal-based MEMS fabricated by micro-electro-discharge machining. *Proceedings of the 20th IEEE Canadian Conference on Electrical and Computer Engineering*, pp. 1-4.
- Takahata, K. & Gianchandani, Y.B. (2008a). A micromachined capacitive pressure sensor using a cavity-less structure with bulk-metal/ elastomer layers and its wireless telemetry application. *Sensors*, Vol. 8, pp. 2317-2330.
- Takahata, K. & Gianchandani, Y.B. (2008b). A cavity-less micromachined capacitive pressure sensor for wireless operation in liquid ambient. *Proceedings of the Solid-State Sensor, Actuator and Microsystems Workshop*, pp. 300-303.
- Takahata, K.; Gianchandani, Y.B. & Wise, K.D. (2006). Micromachined antenna stents and cuffs for monitoring intraluminal pressure and flow. *IEEE/ASME Journal of Microelectromechanical. Systems*, Vol. 15, No. 5, pp. 1289-1298.
- Takahata, K. & Masaki, T. (1999). High precision machining of micro V-grooves. *Proceedings of the Japan Society for Precision Engineering Kansai-Region Annual Meeting*, pp. 35-36.
- Takahata, K.; Shibaïke, N. & Guckel, H. (1999). A novel micro electro-discharge machining method using electrodes fabricated by the LIGA process. *Proceedings of the 12th IEEE International Conference on Micro Electro Mechanical Systems*, pp. 238-243.
- Takahata, K.; Shibaïke, N. & Guckel, H. (2000). High-aspect-ratio WC-Co microstructure produced by the combination of LIGA and micro-EDM. *Microsystem Technologies*, Vol. 6, No. 5, pp. 175-178.
- Takeuchi, H.; Nakamura, K.; Shimizu, N. & Shibaïke, N. (2000). Optimization of mechanical interface for a practical micro-reducer. *Proceedings of the 13th IEEE International Conference on Micro Electro Mechanical Systems*, pp. 170-175.
- Takeda, M.; Namura, K.; Nakamura, K.; Shibaïke, N.; Haga, T. & Takada, H. (2000). Development of chain-type micromachine for inspection of outer tube surfaces (basic performance of the 1st prototype). *Proceedings of the 13th IEEE International Conference on Micro Electro Mechanical Systems*, pp. 805-810.
- Tathireddy, P.; Rakwal, D.; Bamberg, E. & Solzbacher, F. (2009). Fabrication of 3-dimensional silicon microelectrode arrays using micro electro discharge machining for neural applications. *Technical Digest of the 15th IEEE International Conference on Solid-State Sensors, Actuators and Microsystems*, pp. 1206-1209.

- Wada, T. & Masaki, T. (2005) Machining of micro PCD tool using micro EDM process and machining example. *Journal of the Japan Society for Abrasive Technology*, Vol. 49, No. 10, pp. 546-549.
- Yoon, H.J.; Kim, S.Y.; Lee, S.W. & Yang, S.S. (2000). Fabrication of a micro electromagnetic flow sensor for micro flow rate measurement. *Proceedings of SPIE*, Vol. 3990, pp. 264-271.

IntechOpen

IntechOpen



## **Micro Electronic and Mechanical Systems**

Edited by Kenichi Takahata

ISBN 978-953-307-027-8

Hard cover, 386 pages

**Publisher** InTech

**Published online** 01, December, 2009

**Published in print edition** December, 2009

This book discusses key aspects of MEMS technology areas, organized in twenty-seven chapters that present the latest research developments in micro electronic and mechanical systems. The book addresses a wide range of fundamental and practical issues related to MEMS, advanced metal-oxide-semiconductor (MOS) and complementary MOS (CMOS) devices, SoC technology, integrated circuit testing and verification, and other important topics in the field. Several chapters cover state-of-the-art microfabrication techniques and materials as enabling technologies for the microsystems. Reliability issues concerning both electronic and mechanical aspects of these devices and systems are also addressed in various chapters.

### **How to reference**

In order to correctly reference this scholarly work, feel free to copy and paste the following:

Kenichi Takahata (2009). Micro-Electro-Discharge Machining Technologies for MEMS, Micro Electronic and Mechanical Systems, Kenichi Takahata (Ed.), ISBN: 978-953-307-027-8, InTech, Available from: <http://www.intechopen.com/books/micro-electronic-and-mechanical-systems/micro-electro-discharge-machining-technologies-for-mems>

**INTECH**  
open science | open minds

### **InTech Europe**

University Campus STeP Ri  
Slavka Krautzeka 83/A  
51000 Rijeka, Croatia  
Phone: +385 (51) 770 447  
Fax: +385 (51) 686 166  
[www.intechopen.com](http://www.intechopen.com)

### **InTech China**

Unit 405, Office Block, Hotel Equatorial Shanghai  
No.65, Yan An Road (West), Shanghai, 200040, China  
中国上海市延安西路65号上海国际贵都大饭店办公楼405单元  
Phone: +86-21-62489820  
Fax: +86-21-62489821

© 2009 The Author(s). Licensee IntechOpen. This chapter is distributed under the terms of the [Creative Commons Attribution-NonCommercial-ShareAlike-3.0 License](https://creativecommons.org/licenses/by-nc-sa/3.0/), which permits use, distribution and reproduction for non-commercial purposes, provided the original is properly cited and derivative works building on this content are distributed under the same license.

IntechOpen

IntechOpen